ACS Photonics

Letter

pubs.acs.org/journal/apchd5

Optical Detection in a Waveguide Geometry with a Single Metallic Contact

Satoshi Ishii,*[†,§] Shin-ichiro Inoue,[†,‡] Rieko Ueda,[†] and Akira Otomo[†]

[†]Advanced ICT Research Institute, National Institute of Information and Communications Technology, Kobe, Hyogo 651-2492, Japan

[‡]PRESTO, Japan Science and Technology Agency, Kawaguchi 332-0012, Japan

ABSTRACT: A single metallic contact attached to an optical waveguide is used to electrically detect near-infrared guided light through an optical waveguide. The device has a metal−insulator−metal structure, where the difference in the number of excited hot carriers in the top and bottom metallic layers can generate a photocurrent. The simple, compact structure of the device allows it to be integrated with any type of optical waveguide to monitor the guided light.

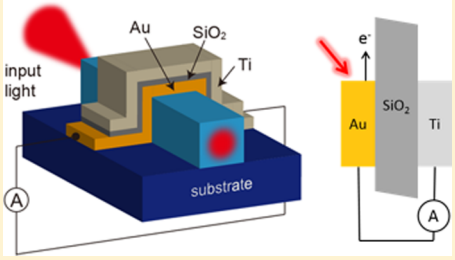

KEYWORDS: *Hot carrier, metal thin film, optical waveguide, internal photoemission*

Recent progress in photonics has occurred faster than for electronics,[1,2] increasing the prominence of photonic devices and photonic systems. This progress is predicted to accelerate over the next few decades. Currently, however, photonic and electronic systems coexist. It is therefore, critical that electronic information can be readily transferred to photonic information and *vice versa*. In this regard, it is important to realize that typically electrons and photons travel through different materials: metallic conducting wires for electrons and optical waveguides made of insulators for photons. The differences in materials used in electronics and photonics pose challenges for constructing compact, integrated optoelectronic and electro-optic devices.

Semiconductor photodiodes are typically used for the photodetection of the optical signals guided through optical waveguides. Using compound semiconductors allows for the monolithic integration of waveguides and photodetectors. However, widely used photonic devices based on silicon and polymers cannot be monolithic. Germanium[3,4] and silicon−germanium[5,6] detectors have been integrated into silicon photonic devices, and various types of photodiodes have been integrated in polymer-based photonic devices.[7] Additional optical components such as mirrors[7,8] and couplers[9] have been integrated into optical waveguides to improve photodetection. In both cases, integration processes can cause complications.

Plasmonic Schottky photodetectors have been developed for use with silicon waveguides.[10,11] A gold contact on a silicon waveguide has been used to form a Schottky contact with a silicon waveguide. The portion of guided light absorbed by the gold contact excites hot electrons, which cross the Schottky barrier to produce a photocurrent. The other end of the gold contact can be wired to an electronic circuit, enabling for the integration of photonic and electronic systems. Plasmonic Schottky contacts have also been used to detect light propagation through free space[12−14] and surface plasmon polaritons guided along plasmonic waveguides.[3,15−18] Plasmonic Schottky photodetectors are one of the simplest ways to detect guided light. However, Schottky contacts can only be formed with semiconductors. Therefore, plasmonic Schottky detectors cannot be applied to polymer waveguides or optical fibers that are made of insulators.

This limitation can be overcome by using a metal−insulator−metal (MIM) contact instead of a single-film metal contact. Internal photoemission has been studied for decades, and the photocurrents generated at MIM structures have been reported in numerous papers.[19−30] If the hot carriers, excited by absorbing light, in one of the metal films reach the other metal film by either crossing the energy barriers or by tunneling, then they contribute to the photocurrent. If both of the metal layers generate hot carriers, then the total photocurrent is the difference between the hot carriers that are traveling in opposite directions. While most studies on the photocurrent in MIM systems have focused on the propagating light in free space, recent studies have revealed that surface plasmon polaritons can efficiently generate photocurrent efficiently.[31,32]

In this letter, we show that a MIM structure is a concise photodetector that can monitor the light guided through an optical waveguide. The evanescent field of the guided light was absorbed by the metal films and generated a photocurrent by internal photoemission. In an analogous manner to the plasmonic Schottky contact in an optical waveguide, the top and bottom metal films that formed the MIM contact could be readily wired to electrical circuits. The photodetector has a

Received: April 21, 2014
Published: October 21, 2014

gold−silica−titanium trilayer, where the gold film was on the bottom, in contact with a polymer waveguide and had photoresponse from visible to near-infrared wavelengths. This device was fabricated using standard photolithography followed by thin film preparation without using semiconductors and could be used for any kind of optical waveguides, regardless of its conductivity.

In this experiment, each sample was prepared in two steps: the polymer waveguides were prepared, followed by the fabrication of the metallic contacts. The polymer waveguides were fabricated on silicon wafers with a 2 μm thick silicon oxide top layer following the standard procedure of SU-8 (Micro-Chem, SU-8, 2002). The cross sections of the SU-8 waveguides were trapezoidal to ensure that the films coated the sides of the waveguides. The top and bottom edges of the waveguides were 5 and 8 μm thick, respectively, and their height was 1.53 μm.

A positive photoresist (Shipley, Microposit S1818) was used to define the position of the metallic contacts. During sputtering, a shadow mask was used to cover one side of the SU-8 waveguide. After the bottom metal film had been sputtered, a second shadow mask was positioned on the other side of the SU-8 waveguide. A silica (SiO_2) layer was then sputtered on top of the first metal layer. Finally, the top metal film was sputtered after the first shadow mask had been removed. A subsequent lift-off process left the metallic structure, which covered the SU-8 waveguides.

The gold, silicon oxide, and titanium films were 25, 10, and 20 nm thick, respectively. The thicknesses and optical properties of the films were confirmed by a spectroscopic ellipsometer (J. A. Woollam, M-2000). The in-plane widths of the trilayer films that covered the waveguide were 5 μm. A schematic diagram of the device and a top-view microscope image taken with a CCD camera are shown in Figure 1.

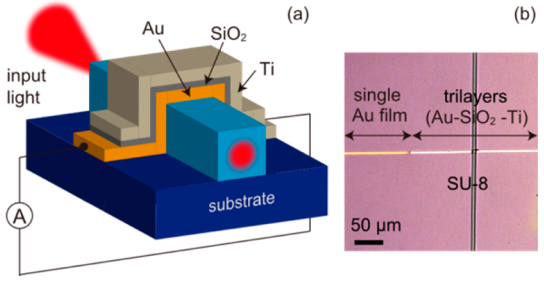

Figure 1. (a) Schematic diagram of the device and (b) a microscope image of the fabricated device, taken near the contact area.

To measure the photocurrent in the device, a waveguide characterization setup equipped with two electrical probes was built. The light from a continuous-wave diode laser was focused on the cleaved end of the waveguide by a 20× objective lens. The illumination power was controlled by neutral-density filters. The device was contacted to probes that were connected to a picoammeter (Keithley 487). The picoammeter measured the current and also applied a bias to the device using its built-in DC source unit. No external amplifiers were used in the electrical measurements. A photocurrent was obtained by subtracting the dark current from the current measured under light illumination.

The following notations were used to describe the flow of the photocurrent and the applied bias in the experiments. The positive photocurrent direction was defined as the photocurrent flowing from the gold film to the titanium film through the load (picoammeter), while the current flowing in the opposite direction was defined as negative. The bias was defined in terms of the Fermi level of the gold film with respect to that of the titanium film. Therefore, applying a negative voltage to the gold film increased its Fermi level in comparison with that of titanium, which was defined as positive.

Figure 2 shows the photocurrent under an applied bias for the sample with different input powers at a wavelength of 680 nm. The photocurrent increased at high positive biases and input power. With a negative bias, the photocurrent was slightly negative and had little dependence on both the input power and the amplitude of the negative bias, within the range tested. When the input power was 0.1 mW, the short-circuit current and open-circuit voltage for the device were 0.7 nA and −0.07 V, respectively. The nonlinear response of the photocurrent with respect to the input power may have been caused by the space-charge limit.[33] The sensitivity of the device was on the order of a few tens of mA/W at 1 V. The low sensitivity was partially caused by the fact that the device only detected the evanescent field of the guided light without blocking the optical waveguide. Optimizing the geometry[34] or changing the combination of materials in the trilayer is expected to dramatically improve the sensitivity of the device.

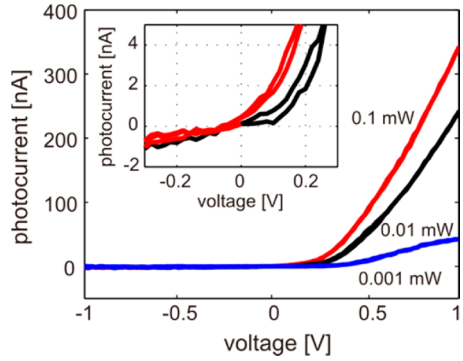

Figure 2. Bias dependence of the device at a wavelength of 680 nm measured at 0.1, 0.01, and 0.001 mW. The inset shows a magnified view of the plot around zero bias at 0.1 and 0.01 mW.

Figure 3 shows the wavelength dependence of the device at a fixed input power of 0.1 mW. Each photocurrent shown in Figure 3b is obtained by subtracting the current measured under light illumination from the dark current shown in Figure 3a. Overall, photocurrents were larger at shorter wavelengths; however, the difference of photocurrent between 680 and 760 nm was minute, and the photocurrent at 1064 nm was much smaller. These dependences of the photocurrents with respect to the wavelengths may have been caused by the effects of two opposing factors: the photon energy and optical absorption. Smaller photon energies resulted in reduced probability of hot electrons to cross the silica barrier. However, the absorption in the gold layer was larger for longer wavelength because of the larger imaginary part of the gold permittivity, which generated more hot electrons with small photon energies. It is believed that the relative strengths of these factors determine the photocurrent at each wavelength, where further quantitative studies are required. In addition, identical measurements were performed at 1550 nm; however, the device did not have a nonzero short-circuit current at 1550 nm within the sensitivity of our electrical measurement system.

dx.doi.org/10.1021/ph500131v | ACS Photonics 2014, 1, 1089−1092

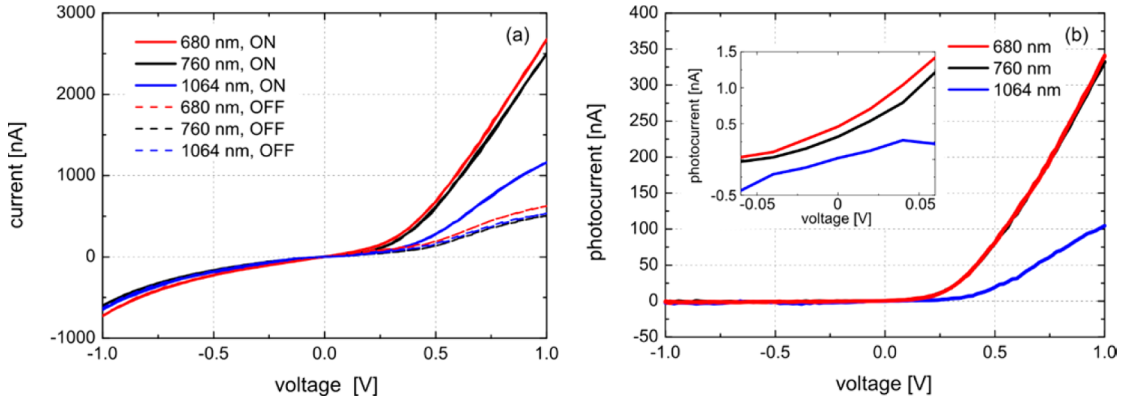

Figure 3. *I*–*V* plots of the raw data measured at 680, 760, and 1064 nm with a power of 0.1 mW. In the legend list, ON refers to the currents measured under light illumination and OFF refers to the dark currents. (b) Photocurrent plots measured at 680, 760, and 1064 nm. Each photocurrent plot is obtained by subtracting the dark current from the current measured under light illumination. The plot measured at 680 nm is identical to that plotted in Figure 2. The inset shows a magnified view of the plot around zero bias.

Numerical simulations were performed to analyze the origin of the photocurrent. Because the band gap of silica is 8.9 eV[35] and the highest photon energy in our experiment was 1.8 eV (680 nm), the observed photocurrent must have been caused by hot carriers generated by internal photoemission in the metal layers. Figure 4a,b shows the mode profiles of the SU-8

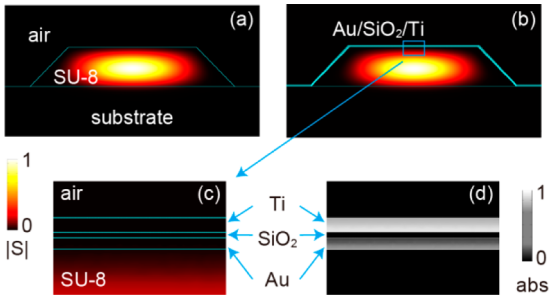

Figure 4. Numerically calculated mode profiles (|S|) of the SU-8 waveguides at 680 nm (a) without a trilayer and (b) with a trilayer. (c) Magnified view of the rectangular area indicated in panel b. (d) Absorption profile (abs) of the area shown in panel c.

waveguide without and with the trilayer, respectively. Figure 4c shows a magnified image of the rectangular area highlighted in Figure 4b. Because the cross section of the waveguide was larger than the single-mode operation, adding a trilayer around the waveguide barely affected the mode profile. The mode indexes without and with a trilayer were 1.5579 and 1.5570 + i9.34 × 10^{-5}, respectively, where the imaginary component came from metallic losses. Thus, only 0.14% of the guided light was absorbed in the trilayer area, which was 5 μm long. The magnified region in Figure 4d shows the amounts of absorption at the metal films, revealing that the titanium film absorbed more strongly than the gold film.

If the number of hot carriers generated was proportional to the amount of absorption in each metal film, then more electrons traveled from the titanium film to the gold film than vice versa, resulting in a net photocurrent flowing from the titanium film to the gold film through the load. However, the measured photocurrent flowed from the gold film to the titanium film at zero bias, as plotted in Figure 2. To clarify the direction of the photocurrent, the electronic structure of the system was considered. The work functions of gold and titanium are 5.2 and 4.2 eV, respectively.[36] As reported in ref 28, the difference in the work functions resulted in a built-in field from the titanium film to the gold film. Thus, electron transport from the gold film to the titanium film was more favorable than in the opposite direction, giving directionality to the photocurrent, as observed in the experiments. A detailed analysis on the photocurrent should include depletion regions at the interfaces as well as the effects of thermal drifts. Also, the electric barriers for hot holes are higher than the electric barriers for hot electrons,[27] and thus the contribution from hot holes in our structure was minor.

In summary, we demonstrated that a MIM contact can detect the guided light through an optical waveguide without blocking the optical pass. The fabrication process of the detector is straightforward and did not require additional heteroepitaxial growth or bonding of semiconducting materials. The detector did not depend on the conductivity of the optical waveguide and could be used with any type of waveguide including polymers and glasses, which are typically processed without semiconductors. By using a gold–silica–titanium trilayer, we were able to detect guided light from 680 to 1064 nm. The sensitivity of the detector and its ability to detect longer wavelengths could be improved by optimizing the materials used and the geometry of the trilayer. Because the photodetector had a small resistance–capacitance delay, it could potentially have a high bandwidth as well as a high-speed response above the GHz range. The dynamic response properties of the detector will be reported in the future.

AUTHOR INFORMATION

Corresponding Author

*E-mail: sishii@nims.go.jp.

Present Address

§International Center for Materials Nanoarchitectonics (MANA), National Institute for Materials Science (NIMS), Tsukuba, Ibaraki 305-0044, Japan.

Notes

The authors declare no competing financial interest.

ACKNOWLEDGMENTS

This work was partially supported by the Ministry of Internal Affairs and Communications under the Strategic Information and Communications R&D Promotion Programme (SCOPE).

REFERENCES

(1) Thylén, L.; He, S.; Wosinski, L.; Dai, D. The Moore's law for photonic integrated circuits. *J. Zhejiang Univ., Sci., A* **2006**, *7*, 1961−1967.

(2) Smit, M.; Van der Tol, J.; Hill, M. Moore's law in photonics. *Laser Photonics Rev.* **2012**, *6*, 1−13.

(3) Ahn, D.; Hong, C.-Y.; Liu, J.; Giziewicz, W.; Beals, M.; Kimerling, L. C.; Michel, J.; Chen, J.; Kńrtner, F. X. High performance, waveguide integrated Ge photodetectors. *Opt. Express* **2007**, *15*, 3916−3921.

(4) Vivien, L.; Osmond, J.; Fedeli, J. M.; Marris-Morini, D.; Crozat, P.; Damlencourt, J. F.; Cassan, E.; Lecunff, Y.; Laval, S. 42 GHz p.i.n Germanium photodetector integrated in a silicon-on-insulator waveguide. *Opt. Express* **2009**, *17*, 6252−6257.

(5) Deimel, P.; Heimhofer, B.; Krotz, G.; Lilienhof, H.; Wind, J.; Muller, G.; Voges, E. Amorphous SiGe: H photodetectors on glass optical waveguides. *IEEE Photonics Technol. Lett.* **1990**, *2*, 499−501.

(6) Splett, A.; Zinke, T.; Petermann, K.; Kasper, E.; Kibbel, H.; Herzog, H. J.; Presting, H. Integration of waveguides and photodetectors in SiGe for 1.3 mm operation. *IEEE Photonics Technol. Lett.* **1994**, *6*, 59−61.

(7) Young, I. A.; Mohammed, E.; Liao, J. T.; Kern, A. M.; Palermo, S.; Block, B. A.; Reshotko, M. R.; Chang, P. L. Optical I/O technology for tera-scale computing. *IEEE J. Solid-State Circuits* **2010**, *45*, 235−248.

(8) Shiraishi, T.; Yagisawa, T.; Ikeuchi, T.; Ide, S.; Tanaka, K. *Cost-Effective on-Board Optical Interconnection Using Waveguide Sheet with Flexible Printed Circuit Optical Engine*. In OSA/OFC/NFOEC, Los Angeles, CA, USA, 2011; IEEE: Los Angeles, CA; p OTuQ5.

(9) Kato, K. Ultrawide-band/high-frequency photodetectors. *IEEE Trans. Microwave Theory Technol.* **1999**, *47*, 1265−1281.

(10) Goykhman, I.; Desiatov, B.; Khurgin, J.; Shappir, J.; Levy, U. Locally oxidized silicon surface-plasmon Schottky detector for telecom regime. *Nano Lett.* **2011**, *11*, 2219−2224.

(11) Goykhman, I.; Desiatov, B.; Khurgin, J.; Shappir, J.; Levy, U. Waveguide based compact silicon Schottky photodetector with enhanced responsivity in the telecom spectral band. *Opt. Express* **2012**, *20*, 28594−28602.

(12) Knight, M. W.; Sobhani, H.; Nordlander, P.; Halas, N. J. Photodetection with active optical antennas. *Science* **2011**, *332*, 702−704.

(13) Knight, M. W.; Wang, Y.; Urban, A. S.; Sobhani, A.; Zheng, B. Y.; Nordlander, P.; Halas, N. J. Embedding plasmonic nanostructure diodes enhances hot electron emission. *Nano Lett.* **2013**, *13*, 1687−1692.

(14) Sobhani, A.; Knight, M. W.; Wang, Y.; Zheng, B.; King, N. S.; Brown, L. V.; Fang, Z.; Nordlander, P.; Halas, N. J. Narrowband photodetection in the near-infrared with a plasmon-induced hot electron device. *Nat. Commun.* **2013**, *4*, 1643.

(15) Neutens, P.; Van Dorpe, P.; De Vlaminck, I.; Lagae, L.; Borghs, G. Electrical detection of confined gap plasmons in metal−insulator−metal waveguides. *Nat. Photonics* **2009**, *3*, 283−286.

(16) Dufaux, T.; Dorfmuller, J.; Vogelgesang, R.; Burghard, M.; Kern, K. Surface plasmon coupling to nanoscale Schottky-type electrical detectors. *Appl. Phys. Lett.* **2010**, *97*, 161110.

(17) Akbari, A.; Tait, R. N.; Berini, P. Surface plasmon waveguide Schottky detector. *Opt. Express* **2010**, *18*, 8505−8514.

(18) Scales, C.; Breukelaar, I.; Charbonneau, R.; Berini, P. Infrared performance of symmetric surface-plasmon waveguide Schottky detectors in Si. *J. Lightwave Technol.* **2011**, *29*, 1852−1860.

(19) Braunstein, A.; Braunstein, M.; Picus, G.; Mead, C. Photoemissive determination of barrier shape in tunnel junctions. *Phys. Rev. Lett.* **1965**, *14*, 219.

(20) Goodman, A. M.; O'Neill, J. J. Photoemission of electrons from metals into silicon dioxide. *J. Appl. Phys.* **1966**, *37*, 3580−3583.

(21) Gundlach, K. H.; Kadlec, J. Spectral dependence of the photoresponse in MIM structures: Influence of the electrode thickness. *Thin Solid Films* **1975**, *28*, 107−117.

(22) Burshtein, Z.; Levinson, J. Photo-induced tunnel currents in Al-Al2O3-Au structures. *Phys. Rev. B* **1975**, *12*, 3453−3457.

(23) Elchinger, G. M.; Sanchez, A.; Davis, C. F.; Javan, A. Mechanism of detection of radiation in a high-speed metal-metal oxide-metal junction in the visible region and at longer wavelengths. *J. Appl. Phys.* **1976**, *47*, 591−594.

(24) Slayman, C.; Guedes, M.; Yee, T.; Gustafson, T. Small Area Metal-Oxide-Metal Junctions As Picosecond Photoemissive Detectors. In *Picosecond Phenomena*; Springer: New York, 1978; pp 186−189.

(25) Diesing, D.; Merschdorf, M.; Thon, A.; Pfeiffer, W. Identification of multiphoton induced photocurrents in metal−insulator−metal junctions. *Appl. Phys. B: Laser Opt.* **2004**, *78*, 443−446.

(26) Kovacs, D. A.; Winter, J.; Meyer, S.; Wucher, A.; Diesing, D. Photo and particle induced transport of excited carriers in thin film tunnel junctions. *Phys. Rev. B* **2007**, *76*.

(27) Thissen, P.; Schindler, B.; Diesing, D.; Hasselbrink, E. Optical response of metal−insulator−metal heterostructures and their application for the detection of chemicurrents. *New J. Phys.* **2010**, *12*, 113014.

(28) Stella, K.; Kovacs, D. A.; Diesing, D.; Brezna, W.; Smoliner, J. Charge transport through thin amorphous titanium and tantalum oxide layers. *J. Electrochem. Soc.* **2011**, *158*, P65−P74.

(29) Wang, F.; Melosh, N. A. Power-independent wavelength determination by hot carrier collection in metal-insulator-metal devices. *Nat. Commun.* **2013**, *4*, 1711.

(30) Powell, R. Interface barrier energy determination from voltage dependence of photoinjected currents. *J. Appl. Phys.* **1970**, *41*, 2424−2432.

(31) Wang, F.; Melosh, N. A. Plasmonic energy collection through hot carrier extraction. *Nano Lett.* **2011**, *11*, 5426−5430.

(32) Pradhan, A.; Holloway, T.; Mundle, R.; Dondapati, H.; Bahoura, M. Energy harvesting in semiconductor-insulator-semiconductor junctions through excitation of surface plasmon polaritons. *Appl. Phys. Lett.* **2012**, *100*, 061127.

(33) Goodman, A. M.; Rose, A. Double extraction of uniformly generated electron-hole pairs from insulators with noninjecting contacts. *J. Appl. Phys.* **1971**, *42*, 2823−2830.

(34) Chalabi, H.; Schoen, D.; Brongersma, M. L. Hot-electron photodetection with a plasmonic nanostripe antenna. *Nano Lett.* **2014**, *14*, 1374−1380.

(35) Bersch, E.; Rangan, S.; Bartynski, R. A.; Garfunkel, E.; Vescovo, E. Band offsets of ultrathin high-κ oxide films with Si. *Phys. Rev. B* **2008**, *78*, 085114.

(36) Michaelson, H. B. The work function of the elements and its periodicity. *J. Appl. Phys.* **1977**, *48*, 4729−4733.